

# Pitfalls and Protocols: Evaluating Catalysts for CO<sub>2</sub> Reduction in Electrolyzers Based on Gas Diffusion Electrodes

*Ying Chuan Tan<sup>1,2,\*</sup>, Wei Kang Quek<sup>3</sup>, Beomil Kim<sup>4</sup>, Sigit Sugiarto<sup>1</sup>, Jihun Oh<sup>4,\*</sup>, Dan Kai<sup>1,2,\*</sup>*

<sup>1</sup> Institute of Materials Research and Engineering (IMRE), A\*STAR, 2 Fusionopolis Way, Innovis, #08-03, Singapore 138634, Singapore

<sup>2</sup> Institute of Sustainability for Chemicals, Energy and Environment (ISCE2), A\*STAR, 2 Fusionopolis Way, Innovis, #08-03, Singapore 138634, Singapore

<sup>3</sup> Department of Material Science Engineering, National University of Singapore, 9 Engineering Drive 1, Singapore 117575, Singapore

<sup>4</sup> Department of Materials Science and Engineering, Korea Advanced Institute of Science and Technology (KAIST), 291 Daehak-ro, Yuseong-gu, Daejeon 34141, Republic of Korea

## AUTHOR INFORMATION

### Corresponding Authors

\*Ying Chuan Tan; Email: [tan\\_ying\\_chuan@isce2.a-star.edu.sg](mailto:tan_ying_chuan@isce2.a-star.edu.sg).

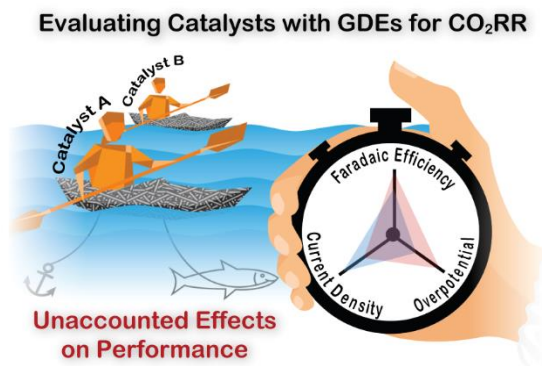
\*Jihun Oh; Email: [jihun.oh@kaist.ac.kr](mailto:jihun.oh@kaist.ac.kr).

\*Dan Kai; Email: [kaid@imre.a-star.edu.sg](mailto:kaid@imre.a-star.edu.sg).

## ABSTRACT

The evaluation of catalysts on gas diffusion electrodes (GDEs) have propelled the progress of electrochemical CO<sub>2</sub> reduction reaction (CO<sub>2</sub>RR) at industry-relevant activities. However, high experimental complexities exist in GDE-based flow electrolyzers, whereby various experimental factors can influence the evaluation of catalytic CO<sub>2</sub>RR performances. Without accounting for these experimental factors could result in inconsistent conclusions and thus hinder rational catalyst developments. This Perspective highlights a range of experimental factors that can affect the performance metrics for electrocatalysts. Specifically, the product faradaic efficiency can be influenced by the overestimation of the effluent gas flow rate, unaccounted losses of products and unintended alteration of microenvironments. In addition, cathodic voltage can be inaccurately determined due to the unaccounted dynamic changes in uncompensated resistance. By raising awareness of these potential pitfalls and establishing appropriate protocols, we foresee a more meaningful benchmarking of catalytic performances across literatures.

## TOC GRAPHICS



CO<sub>2</sub> electrolysis is an emerging approach to electrify the synthesis of chemicals and fuels from CO<sub>2</sub>.<sup>1-3</sup> Coupled with low-carbon sources of electricity, CO<sub>2</sub> electrolysis can potentially reduce carbon emissions while providing economic value.<sup>4</sup> In contrast to high-temperature CO<sub>2</sub> electrolyzer,<sup>5</sup> electrochemical CO<sub>2</sub> reduction reaction (CO<sub>2</sub>RR) in low-temperature electrolyzers have demonstrated the unique ability to produce valuable multicarbons (products with two or more carbon atoms; denoted as C<sub>2+</sub>).<sup>6, 7</sup> Catalyst development plays a key role in advancing CO<sub>2</sub>RR technology as catalysts could control product selectivity while reducing overpotentials.<sup>1, 8-12</sup> At the same time, the pursuit toward economic feasibility for CO<sub>2</sub>RR relies on the designs of electrodes to intensify the process.<sup>13</sup> Particularly, gas diffusion electrodes (GDEs) are essential for attaining industry-relevant activities by enhancing the mass transport of CO<sub>2</sub> reactants.<sup>14-18</sup> Furthermore, the microenvironments of the catalyst surfaces in GDE-based electrolyzers are more similar to industrial electrolyzers as compared to conventional H-type cells.<sup>19</sup> Hence, there has been an increasing focus on benchmarking catalysts using electrolyzers based on GDEs, and thus a rapid progress in CO<sub>2</sub>RR performance has been demonstrated.<sup>11, 14, 20, 21</sup> For example, production of C<sub>2+</sub> molecules at ampere-level current densities have recently been achieved, which are comparable with the activities in industrial water electrolyzers.<sup>22, 23</sup>

Despite the rapid progress of electrocatalyst development demonstrated with GDE-based flow electrolyzers, there are still some inconsistencies between reported studies. Specifically, pure Cu catalysts, which are often used as control samples in individual studies, can exhibit performances that vary widely across different literature reports. For example, in the same electrolyte system, sputtered Cu thin films on similar PTFE-based GDE substrates had demonstrated differing C<sub>2</sub>H<sub>4</sub> Faradaic efficiencies (FEs) and C<sub>2</sub>H<sub>4</sub> partial current densities from ~20–45% and ~10–100 mA cm<sup>-2</sup>, respectively, at -1.1 V *vs* RHE (Figure 1a).<sup>23-27</sup> The presence of such discrepancies in baseline-performance among control samples suggests that it is not always meaningful to compare newly developed catalysts (Figure 1b) with previous reports. Such inconsistencies are due to the presence of numerous experimental factors that can contribute to the observed catalytic performance.<sup>28-30</sup> When an experimentalist is unaware and thus does not address these contributing factors, one could experience an inaccurate determination of product FEs and cathodic voltages (Figure 1c). These experimental pitfalls, though already reported, have received less attention in the research community as compared to the development of state-of-the-art catalysts.

In this Perspective, we will summarize various sources of experimental pitfalls that can impact the accuracy of performance evaluation for CO<sub>2</sub>RR. In particular, the product faradaic efficiency can be affected by the overestimation of effluent gas flow rate, unaccounted losses of products and unintended alteration of microenvironments. On the other hand, cathodic voltage can be inaccurately determined due to the unaccounted dynamic changes in uncompensated resistance. At the same time, suitable protocols will be highlighted to address these issues. Specifically, the list of pitfalls and protocols will be applicable to three-compartment GDE-based flow electrolyzers, which enable convenient three-electrode measurement for catalyst evaluation. Among these examples, we will focus on catalytic systems for the electrosynthesis of multi-carbon products (*e.g.* ethylene, ethanol, 1-propanol) as these products have great global market size (> \$300B) and potential impact on decarbonization (> 1.4 GT CO<sub>2</sub> equivalent of emission reduction).<sup>4</sup>

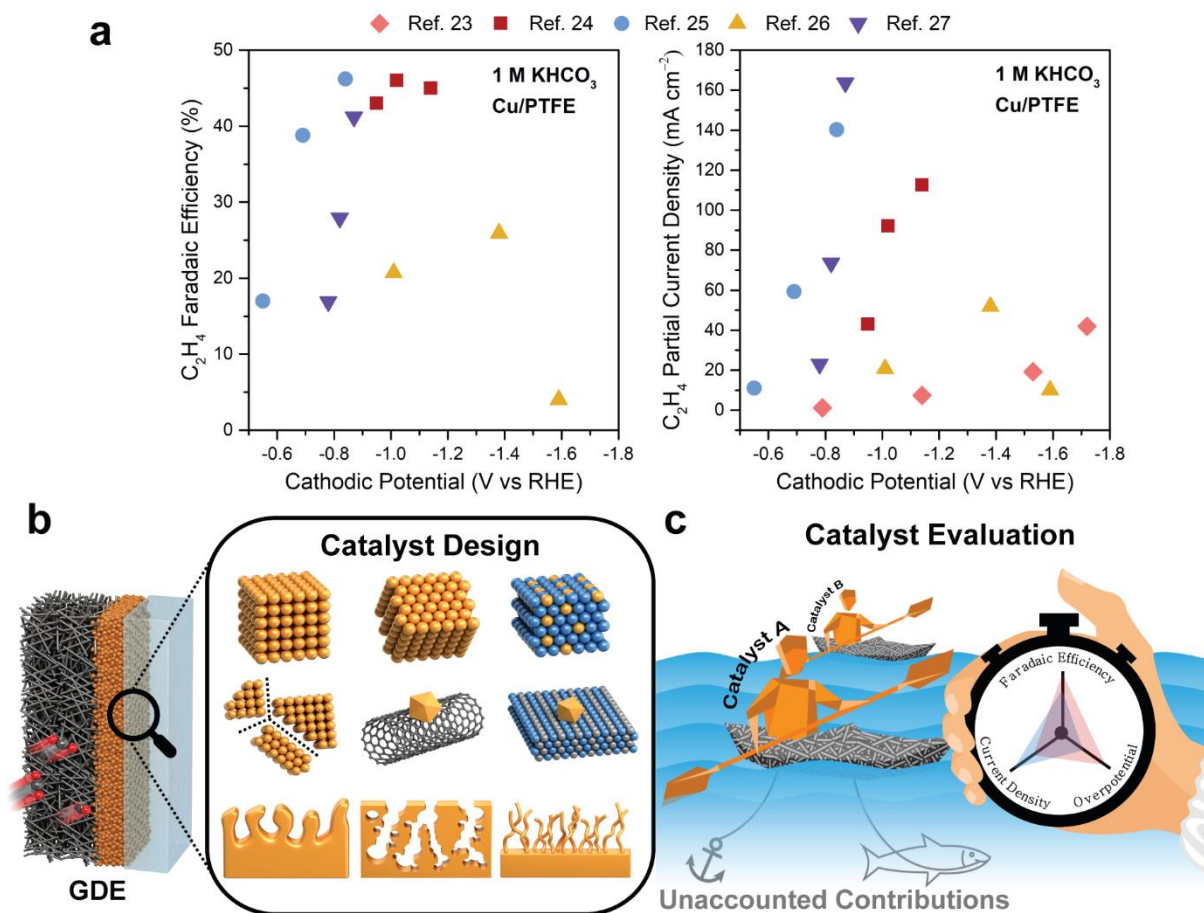


**Figure 1.** (a) Comparison of previously reported CO<sub>2</sub>RR performance of Cu catalysts deposited on PTFE GDE substrates, which had been used as control samples for each study, in 1 M KHCO<sub>3</sub> electrolyte (see Table S1 in Supporting Information for the specific literature data). Schematic

illustrations of (b) the typical design strategies of electrocatalysts for enhancing CO<sub>2</sub>RR, and (c) the evaluation of catalysts based on performance metrics, which can be affected by unaccounted experimental contributions. The paddlers and kayaks signify the catalysts and GDEs, respectively, while their performance is measured by a stopwatch. The unaccounted contributions are represented by the anchor and fish hidden below the surface of the water that could slow down or speed up the kayak, respectively, without being noticed by the evaluator.

## IMPORTANCE OF GDES

Conventionally, CO<sub>2</sub>RR has been investigated in aqueous-fed electrolyzers, such as H-type cells and sandwiched cells, in which CO<sub>2</sub> reactants are dissolved and transported through the liquid electrolyte (Figure 2a).<sup>31</sup> The low CO<sub>2</sub> solubility as well as the sluggish CO<sub>2</sub> mass transport across the diffusion boundary layer render aqueous-fed electrolyzer unsuitable for industrial use.<sup>31</sup> On the other hand, gas-fed electrolyzer utilizes GDE to overcome the mass transfer limitations by transporting gaseous CO<sub>2</sub> directly to the gas-electrolyte-catalyst interface, thus effectively reducing the diffusion length for dissolved CO<sub>2</sub> to reach the entire catalyst layer (CL).<sup>13, 31</sup> As a result, gas-fed electrolyzer can maintain a sufficiently high local CO<sub>2</sub> concentration to attain high current densities of at least 200 mA cm<sup>-2</sup> that are essential for commercial CO<sub>2</sub>RR application.<sup>14, 15, 32</sup> Such enhancement in CO<sub>2</sub> mass transport has been quantitatively demonstrated using 1D and 2D diffusion-reaction models.<sup>33-35</sup> These numerical models have also suggested that CO<sub>2</sub>RR in GDEs largely occur at the double-phase boundaries, *i.e.* catalyst-electrolyte interfaces (10–1000 nm away from the gas-liquid interface), instead of triple-phase boundaries.<sup>33, 34</sup>

There are mainly two types of gas-fed electrolyzers: catholyte flow electrolyzer (Figure 2b) and the polymer electrolyte membrane electrolyzer, *i.e.* membrane electrode assembly (MEA) electrolyzer (Figure 2c). Due to the use of polymer electrolyte, MEA electrolyzers require the supply of humidified CO<sub>2</sub> feed to facilitate sufficient flux of H<sub>2</sub>O, a proton donor, to the catalyst surface. The gas-fed flow electrolyzer, which is a type of three-compartment cell, is the more convenient choice for the evaluation of electrocatalysts due to a more accessible placement of reference electrode at the liquid catholyte to obtain the cathodic half-cell voltage (Figure 2d).<sup>36</sup> In contrast, the integration of reference electrode in MEA is challenging, thus the electrochemical measurement is typically limited to full-cell voltages.<sup>37</sup> Furthermore, MEA electrolyzers are more expensive to operate than catholyte flow electrolyzers.<sup>36</sup> Apart from the higher cost of commercially available MEA electrolyzers, greater amount of catalysts and an additional current

booster module for the potentiostat are required due to the larger electrode size (typically 5 cm<sup>2</sup> vs 1 cm<sup>2</sup>).

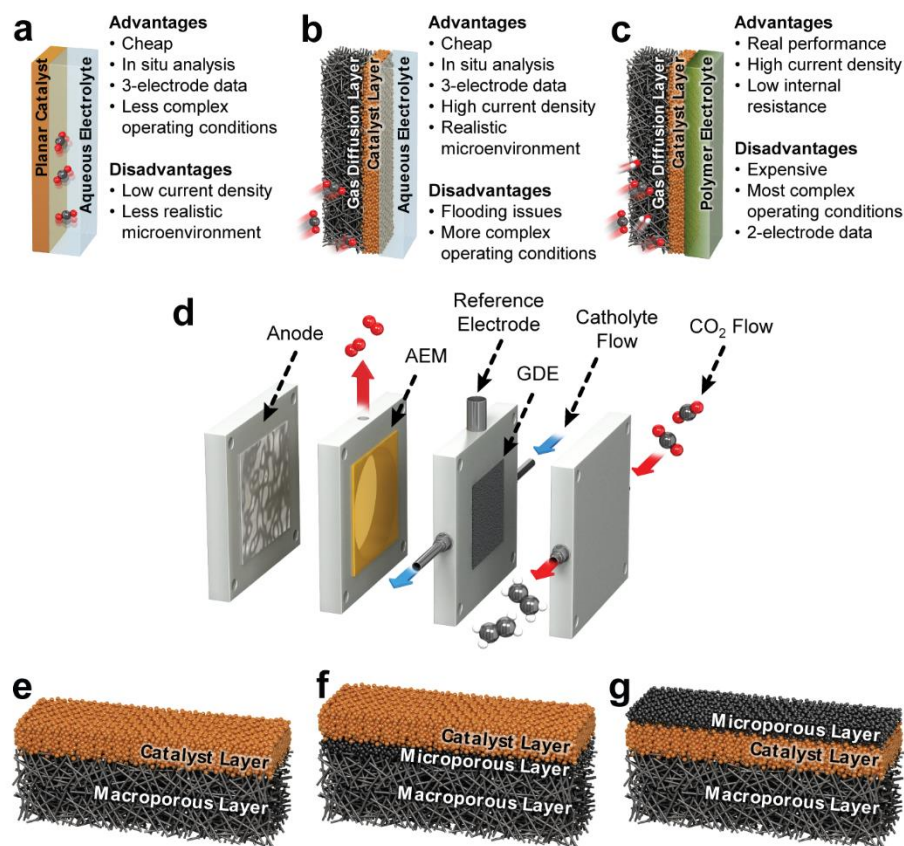


**Figure 2.** Simplified schematic illustrations of various CO<sub>2</sub>RR electrolyzer configurations: (a) aqueous-fed cell, (b) GDE-based flow cell, and (c) GDE-based polymer electrolyte membrane cell. (d) A typical representation of the components that are present in a GDE-based flow cell. AEM: anion-exchange membrane. (e–g) Commonly used structural configurations of catalyst-loaded GDEs.

Typically, GDEs consist of a catalyst layer (CL) and a gas diffusion layer (GDL), which can exist as single or dual layers (Figure 2e,f). A single-layered GDL refers to a GDL with a macroporous substrate (MPS) while a dual-layered GDL has both MPS and microporous layer (MPL).<sup>31</sup> Dual-layered GDLs are usually preferred as the properties of the individual layers can be tuned to optimize the overall conductivity, hydrophobicity and gas permeance. Carbon-based GDLs, that are designed for fuel cells, have been commonly utilized due to their commercial availability,<sup>28,38-40</sup> though porous polytetrafluoroethylene (PTFE) membranes have been actively explored as an alternative GDL because of the enhanced hydrophobicity to prevent flooding issues.<sup>41</sup> Since PTFE

is electrically non-conductive, an additional conductive MPL is added on top of less conductive catalysts, such as metal oxides/sulfides, metal–organic frameworks, etc., to provide better electrical contact with the current collector (Figure 2g). On the other hand, if the catalyst of interest is conductive, *e.g.* sputtered Cu thin film, no additional MPL layer will be required, thus the structural configuration of the GDE will be similar to that shown in Figure 2e.

Performing CO<sub>2</sub>RR with a GDE-based flow electrolyzer enables a more realistic evaluation of catalyst performance under conditions relevant to industrial activities.<sup>19</sup> Unlike the typical H-cell configuration, gas-fed systems exhibit different mass transport characteristics, thus present a distinct microenvironment near the catalyst surfaces that can influence the electrochemical performance and reaction pathway in CO<sub>2</sub>RR and hydrogen evolution reaction (HER). Specifically, the local concentration of CO<sub>2</sub> and OH<sup>-</sup> are considerably higher, which can affect the carbonaceous product selectivity and activity.<sup>19, 42</sup> Even though the rate of CO<sub>2</sub> consumption is higher due to a larger current density, the high local CO<sub>2</sub> concentration can be sustained due to a significantly shorter diffusion path. On the other hand, CO<sub>2</sub>RR is coupled with the production of OH<sup>-</sup>, hence a higher current density enabled by GDEs will result in a higher pH near the surfaces of the catalyst. Therefore, evaluating catalyst performance using a GDE has been increasingly crucial to provide more practical insights to expedite the progress of CO<sub>2</sub>RR technology toward commercialization.

## **PITFALLS**

Although GDE-based flow electrolyzers enable a meaningful catalyst evaluation at industry-relevant activities, a higher experimental complexity exists as compared to H-type cells. These experimental factors can influence the catalytic CO<sub>2</sub>RR evaluation, hence they are considered as pitfalls if left unaccounted. Establishing protocols to eliminate/reduce these contributing factors during CO<sub>2</sub>RR can thus enable a more meaningful comparison of catalysts across literatures and laboratories.

### **Factors Affecting FEs of Products.**

Other than the effect of catalyst properties, experimental factors can affect the determination of product FEs as well (Figure 3). The FE of a specified product is typically calculated from the following equation:

$$FE_i (\%) = \frac{n_i z_i F}{Q} \times 100, \quad (1)$$

where  $n_i$  is the number of moles of the product (gas product: product concentration  $\times$  gas flow rate  $\times$  period of measurement; liquid product: product concentration  $\times$  volume of electrolyte);  $z_i$  is the number of electrons required to generate the product (2 for the formate, carbon monoxide and hydrogen; 6 for methanol; 8 for methane and acetate; 12 for ethylene and ethanol; and 18 for 1-propanol);  $F$  is the Faraday's constant ( $96,485 \text{ C mol}^{-1}$ );  $Q$  is the amount of charge passed during the measurement. Theoretically, FEs for all accounted products will add up to 100% for the overall charge to be balanced in the system. However, this is not a sufficient criterion to determine the accuracy of an electrochemical test for a GDE-based system due to a wide variety of contributing factors that will be discussed below.

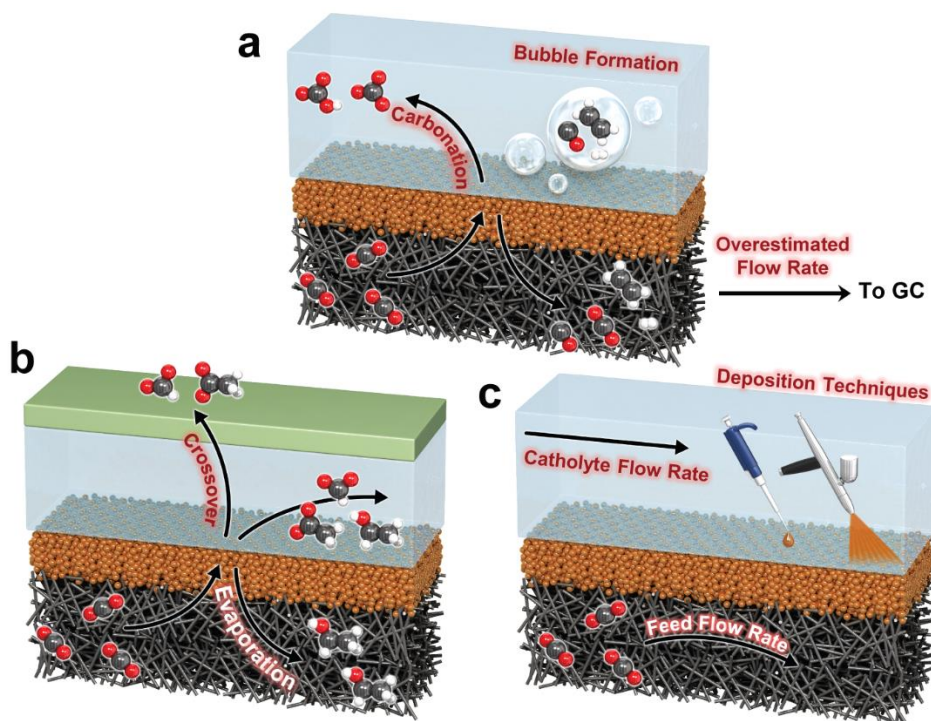


**Figure 3.** Common pitfalls that affect product FEs when evaluating CO<sub>2</sub>RR with GDE-based flow electrolyzers. (a) Overestimation of effluent gas flow rate used for FE determination due to a



decrease in actual gas flow rate. (b) Unaccounted losses of products. (c) Unaccounted alteration of microenvironment from experimental factors.

Considering that charge measurement can be accurately performed with typical potentiostats, systematic errors involved in the determination of FEs are usually originated from the measurement of  $n_i$ , which is a function of product concentration and flow rate (for gas products). For example, Liu *et al.* reported that due to the higher gas product concentration generated from the high production rate in GDE flow cells, an overestimation of gas concentration could be resulted if the obtained concentration is outside of the calibration range.<sup>28</sup> This is because the gas chromatography (GC) peak area may not vary linearly at high concentration. Therefore, conducting a proper calibration range and choosing an optimized split injection condition are recommended for experiments dealing with high current densities and/or high single-pass conversions.

The calculated  $n_i$ , and thus FEs, of gas products in Equation 1 could also be wrongly determined if the gas flow rate is inaccurately used. In an H-type cell with CO<sub>2</sub>-saturated bicarbonate electrolyte, the inlet gas flow rate can be used since the consumption rate of CO<sub>2</sub> and production rate of gas products can be insignificant. However, the use of inlet gas flow rate fed to GDE-based electrolyzers for the calculation in Equation 1 could lead to a significant overestimation of gas products FE due to a vastly different flow rate at the outlet stream (Figure 3a). This is especially serious when alkaline electrolytes are employed as OH<sup>-</sup> will readily react with the CO<sub>2</sub> reactants to form carbonates/bicarbonates.<sup>29, 43, 44</sup> Alkaline electrolytes, such as KOH (1–10 M), have been commonly used to suppress CH<sub>4</sub> production while promoting ethylene production,<sup>41</sup> though the latter effect still debatable.<sup>29, 45</sup> Seger's team showed that other than the CO<sub>2</sub>RR reaction by the catalyst, around 70% of the consumed reactant CO<sub>2</sub> are involved in the undesired carbonation reaction.<sup>29</sup> Furthermore, the authors showed that when the actual outlet gas flow rate is not accounted for, the overestimation of the gas product FEs can be up to 1.64 times higher than the actual value (Figure 4a). Considering that operating the electrolyzer at high current densities would also yield a high local pH at the cathode even with neutral buffers, special care in accounting for the outlet flow rate should also be performed in KHCO<sub>3</sub> electrolytes.

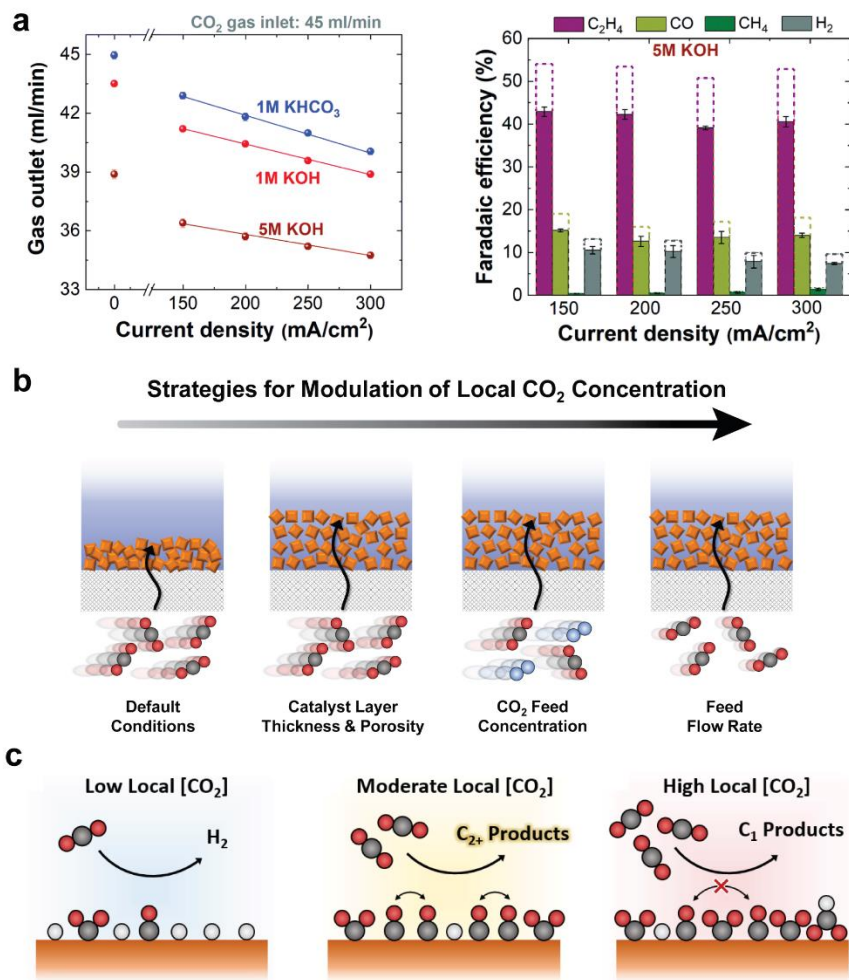


**Figure 4.** (a) Effect of unaccounted changes in gas flow rate on the determined FEs of gaseous products. Reprinted with permission from ref 29. Copyright 2020 Royal Society of Chemistry. (b,c) A range of operational parameters that affects the local CO<sub>2</sub> concentration, which in turn influences the surface coverage of intermediates and thus reaction pathways. Reprinted with permission from ref 42. Copyright 2020 Elsevier.

Another common systematic error involves the crossovers of liquid CO<sub>2</sub>RR products, which if unaccounted, would cause the FE of these products to be underestimated (Figure 3b). Ideally, the liquid products should solubilize and remain in the catholyte reservoir. In reality, however, some liquid products can pass through the GDE and anion-exchange membrane (AEM), resulting in an underestimated product concentration.<sup>46, 47</sup> For example, Zhang *et al.* reported a 36.3% and 46.7% loss of ethanol and 1-propanol, respectively, at 300 mA cm<sup>-2</sup> via vaporizing and passing through the GDE to the gas chamber.<sup>46</sup> On the other hand, the concentration of non-volatile products, such as formate, could be underestimated by 17%–30% as these anionic products can pass through the

AEM by electromigration and end up in the anode chamber. More products will crossover with increasing current density due to four factors.<sup>46</sup> First, under high current density, concentration of products is higher and since the crossover rate is directly proportional to the product concentration, crossover of products increases with high current density. Secondly, the increasing current density relates to a higher cell potential, which leads to an increase in electromigration rate as well as a decrease in electro-osmotic drag. Thirdly, the increased formation rate of gaseous products at higher current density results in the faster convective evaporation of liquid products thereby promoting the crossover of volatile liquid products. Last, a higher current density would lead to higher ohmic heating and an increase in catholyte temperature. The increased temperature not only enhances the evaporation of volatile products, such as ethanol and 1-propanol, but it also affects the reaction kinetics and thus the catalytic performance.

Apart from the losses of liquid products, gaseous reactants and products can also crossover through the GDE and escape *via* the catholyte effluent as bubbles (Figure 3a).<sup>48</sup> As a result, the gas product determined from GC measurement would also be underestimated. Specifically, Niu *et al.* reported that the loss of gas products through bubbles in the catholyte was more serious at higher current density, *i.e.* total gas FEs decreased from 77.8% to 46.3% at 500 mA cm<sup>-2</sup>. However, it is important to note that the extent of losses of gas products depends on the bubble management which varies across different system parameters, such as electrolyte flow rate, structure of catalyst layer, GDE substrate, etc.<sup>48</sup>

Microenvironment, *i.e.* the local environment near the catalyst surface, have been employed as a useful tool to steer the reaction pathways, thus influencing the catalytic CO<sub>2</sub>RR.<sup>49</sup> Hence, maintaining similar microenvironments between experimental studies is essential for a proper comparison of electrocatalyst performance. For example, the choice of cations and anions in electrolytes has significant effects on the microenvironment.<sup>50-56</sup> Therefore, most researchers are aware that the evaluation of catalysts should be performed in commonly used electrolyte systems, such as 1 M KHCO<sub>3</sub> and 1 M KOH, to enable comparison across studies with the same electrolyte. However, there are other experimental factors that affect the microenvironment, which are not always accounted for (Figure 3c).

The catholyte flow rate in a GDE-based flow electrolyzer is an extrinsic factor that can affect the FE of CO<sub>2</sub>RR products. Increasing the electrolyte flow rate enhances the diffusion mass transfer of ions and molecules by shortening the diffusion boundary layer. Therefore, the microenvironment can be influenced by the catholyte flow rate. For example, in an alkaline electrolyte system, a higher catholyte flow rate can lower the concentration of carbonates near the catalyst, thus maintaining a high local pH and high electrolyte conductivity.<sup>57</sup> At the same time, the authors suggested that a higher electrolyte flow rate could also facilitate the desorption of CO, which was proposed to be rate-limiting. Therefore, the production of CO was demonstrated to be enhanced at higher electrolyte flow rates. However, we believe that a higher electrolyte flow rate could also play a role in the removal of bubbles in the electrolyte, which reduces the bubble-induced uncompensated resistance (to be discussed in the next section).<sup>30</sup> Additionally, it is important to note that a high flow rate could also lead to a higher pressure drop, and thus a higher fluid pressure in the catholyte chamber. Consequently, the pressure imbalance between the catholyte and gas chambers could cause flooding and instability issues.<sup>58</sup>

While evaluating an electrocatalyst, it is essential that the supply of CO<sub>2</sub> does not get obstructed over time to maintain a consistent microenvironment. GDEs can sometimes suffer from stability issues, such as the loss of hydrophobicity and the formation of carbonate precipitates.<sup>39</sup> As the pores in GDEs are obstructed by liquid or carbonate crystals, the local CO<sub>2</sub> concentration will decrease and result in the promotion of HER.<sup>59</sup> Therefore, considerable efforts have devoted to investigating the GDE degradation process and improving the stability of GDEs.<sup>60-62</sup> For example, Xu *et al.* proposed a way to minimize the effects of carbonates in GDE with intermittent regeneration voltage, which allows carbonate ions (HCO<sub>3</sub><sup>-</sup>) formed to be transported to the anode.<sup>63</sup> On the other hand, Endrődi *et al.* suggested an intermittent flushing of 25 v/v% isopropanol aqueous solution to remove salt precipitates in GDEs.<sup>64</sup> Although these two studies have shown to greatly improve the long-term performance of GDE-based electrolyzers, the loss of CO<sub>2</sub> reactants through carbonation still persists, thus resulting in additional costs and energy penalty.<sup>44</sup> In this regard, performing CO<sub>2</sub>RR in an acidic environment is believed to prevent the undesired carbonation, therefore improving the stability and economics of GDE-based systems.<sup>65-67</sup> Alternatively, alkaline electroreduction of CO-to-C<sub>2+</sub> has been proposed to avoid carbonation issues, in which the CO feed can be produced from acidic CO<sub>2</sub> electrolyzers or high-temperature solid oxide electrolyzers.<sup>68</sup>

Even though maximizing CO<sub>2</sub> availability is important for minimizing HER, Tan *et al.* reported that the catalytic C–C coupling is optimal at moderate level of CO<sub>2</sub> concentration at the catalyst microenvironment (Figure 4b,c).<sup>42</sup> It is hypothesized that the local CO<sub>2</sub> concentrations can affect the steady-state adsorbate coverage, *i.e.* \*CO<sub>2</sub>, \*H, and \*CO, which in turn affects the reaction pathway (Figure 4c). Conversely, with a high local CO<sub>2</sub> concentration, the high surface coverage of adsorbates may also cause adsorbate-adsorbate repulsion of \*CO, which weakens the bond between carbon and Cu, thereby possibly leading \*CO to desorb prematurely.<sup>42, 69</sup> Consequently, this finding establishes that experimental factors that affects the local CO<sub>2</sub> concentration can in turn influence the catalytic pathway in CO<sub>2</sub>RR.

The CO<sub>2</sub> flow rate can also affect the catalyst performance as it alters the local CO<sub>2</sub> concentration.<sup>42</sup> The change in flow rate causes the gas diffusion boundary layer thickness to vary accordingly, which in turn results in a change in the local CO<sub>2</sub> concentration. The flow rate also determines the average partial pressure of CO<sub>2</sub> in the gas chamber due to the dilution effect from the gaseous products. At a moderate CO<sub>2</sub> flow rate, the C<sub>2+</sub> product FE is the highest while the C<sub>1</sub> product FE is at a minimum. Higher CO<sub>2</sub> flow rate results in higher C<sub>1</sub> product FE at the expense of C<sub>2+</sub> product FE, while a low CO<sub>2</sub> flow rate increases H<sub>2</sub> FE at the expense of C<sub>2+</sub> FE.<sup>42</sup> Recently, Fenwick *et al.* also highlighted that the gas flow rate can affect the wetted state of Au catalyst layer.<sup>70</sup> A lower CO<sub>2</sub> flow rate led to a high portion of wetted catalyst surface, which caused a decrease in CO selectivity. Therefore, this work also suggests a decrease in CO<sub>2</sub> flow would reduce the local CO<sub>2</sub> concentration, thus affecting the reaction pathway for copper-based catalysts.

The deposition technique for the fabrication of catalyst layers on GDEs is another experimental factor that can affect the microenvironment during CO<sub>2</sub>RR (Figure 3c).<sup>42</sup> Even with a fixed catalyst loading, the deposition procedure can alter the thickness of catalyst layers, which affects the local CO<sub>2</sub> concentration (Figure 4b) and thus influences the selectivity toward C<sub>2+</sub> products as discussed above. More specifically, deposition techniques in which the solvent evaporates more rapidly, such as air-brushing, gives a thicker and uniform catalyst layer. On the other hand, deposition techniques with slower solvent evaporation rate, such as dropcasting and hand-painting, will have some catalyst ink leaking into the microporous layer, yielding a thinner and less uniform catalyst layer. Tan *et al.* demonstrated that air-brushing is the more superior deposition technique, with a C<sub>2+</sub> FE of 45% as compared to 25% using the dropcasting technique at 200 mA cm<sup>-2</sup>.<sup>42</sup> A similar

trend was also observed when the temperature of deposition environment was varied; a higher deposition temperature (50 °C – 75 °C) led to a thicker catalyst layer and thus a higher C<sub>2+</sub> FE as compared to that prepared at room temperature. Furthermore, Berlinguette's team had also highlighted that the choice of solvent for the catalyst ink can also affect the performance in CO<sub>2</sub>RR.<sup>71</sup> In particular, the solvent controls the aggregation of the ionomer, which in turns influence the structure and properties of the catalyst layer, thus altering the microenvironment of the catalyst surfaces. In the reported work, ethanol was found to be the optimal solvent for the catalyst/ionomer dispersion system studied.

The choice of polymeric ionomers has also shown to affect CO<sub>2</sub>RR activities. Sargent's team proposed that perfluorinated sulfonic acid ionomers, such as Nafion, can enable an optimal gas and ion transport due to the hydrophobic and hydrophilic properties.<sup>23</sup> Indeed, with a 2-D mass transport model, CO<sub>2</sub> concentration near the catalyst surface can be enhanced due to a more rapid diffusion of the reactants along the ionomer. Consequently, the authors demonstrated that Nafion-coated Cu catalysts could achieve a remarkable ethylene partial current density of 1.3 A cm<sup>-2</sup> in 7 M KOH.<sup>23</sup> However, Nafion is a commonly used ionomer in electrocatalysis, including CO<sub>2</sub>RR, and prior report of ampere-level current density was not observed. Recently, a study by Strasser's group showed that Nafion actually hinders mass transport of CO<sub>2</sub>.<sup>72</sup> This observation is also consistent with another report by Lees *et al.*, which showed that low Nafion content is optimal for their system.<sup>73</sup> These opposing observations have been validated with oxygen reduction reaction, which provides information about the mass transport of gaseous reactants.<sup>23, 72</sup> The reason behind the contradiction is still unclear, though we believe it could be attributed to the use of different GDE substrates; PTFE GDE vs carbon GDE. For example, for the benefits of Nafion to take effect, the ionomer-catalyst layer could require a direct contact with the gas-liquid interface, which may be a challenge in carbon GDEs.<sup>74</sup> Recently, Bell and coworkers proposed a bilayer coating of cation- and anion-conducting ionomers on Cu to regulate the microenvironment, *i.e.* local concentration of OH<sup>-</sup>, H<sub>2</sub>O and CO<sub>2</sub>, to favor the production of multicarbon molecules.<sup>75</sup> Nevertheless, the beneficial effect of this strategy in a GDE system has yet to be demonstrated.

### **Factors Affecting the Cathodic Potentials.**

Typically, the cathodic potentials required to achieve specific current densities are determined to obtain the reaction overpotentials, which is an important measure of the catalyst efficiency. An important step to determine the real working potential is the correction of voltage drop ( $iR$ -drop) from the measured potentials, such as with the following equation for Ag/AgCl reference electrode (saturated KCl):

$$E_{\text{RHE}} = E_{\text{Ag/AgCl}} + 0.197 + 0.0591 \times \text{pH} + I \times R_{\text{u}} \quad (2)$$

Conventionally, electrochemical testing in H-type cells uses the following procedure: (1) measure uncompensated resistance ( $R_{\text{u}}$ ), (2) perform chronoamperometry with potentiostat-compensated  $R_{\text{u}}$  at 85%, (3) manually correct the remaining 15%  $R_{\text{u}}$  after the measurement.<sup>76</sup> Such a protocol assumes that  $R_{\text{u}}$  remains constant throughout the chronoamperometry measurement, which can be valid for low-current situations. However, a high-current environment in GDE flow electrolyzers would experience changes in  $R_{\text{u}}$ . Furthermore, considering that currents are usually above 0.2 A, inaccurate use of  $R_{\text{u}}$  would result in significantly deviated  $iR$ -drop-free overpotentials, *i.e.* an inflated  $R_{\text{u}}$  value of 0.5  $\Omega$  would result in an underestimation of overpotentials by at least 0.1 V.

During  $\text{CO}_2\text{RR}$ ,  $\text{OH}^-$  is produced at the cathode. Hence, at high current density ( $> 50 \text{ mA cm}^{-2}$ ), buffered electrolytes have shown to break down, which leads to a high local pH.<sup>19</sup> As the ionic strength of  $\text{OH}^-$  is higher, the overall electrolyte conductivity between the working and reference electrode increases. At the same time, an increase in electrolyte temperature due to a more pronounced ohmic heating under higher current environment causes a further increase in electrolyte conductivity. Consequently, a lower solution resistance could be observed during electrolysis as compared to that before electrolysis in a GDE-based flow cell (Figure 5a). For example, with 1 M  $\text{KHCO}_3$  electrolyte, Burdyny and coworkers observed a decrease in  $R_{\text{u}}$  by  $\sim 0.7 \Omega$  at a current density of 200  $\text{mA cm}^{-2}$  and the decrease of  $R_{\text{u}}$  will be more pronounced at even greater current densities.<sup>28</sup> Considering that typical overpotential required to reach a total current of 0.2 A (electrode size: 1  $\text{cm}^2$ ) is in the range of 0.5–1.5 V (Figure 1a), an underestimation of overpotential by 0.14 V is substantial. On the other hand, when KOH electrolyte is used, the constant consumption of  $\text{OH}^-$  (higher molar conductivity) through acid-base reaction with  $\text{CO}_2$  would create an accumulation of bicarbonate/carbonate (lower molar conductivity) in the electrolyte. As a result,  $R_{\text{u}}$  increases over time, of which the rate of increase depends on the volume

of the electrolyte reservoir. Nonetheless, this effect could be negated as the current density increases, which creates a consistently high local pH that results in a decrease in  $R_u$ . On the same note, an accumulation of liquid products in the catholyte could also affect the solution resistance. Therefore, it is not advisable to use the original measured  $R_u$  for the correction of voltage drop.

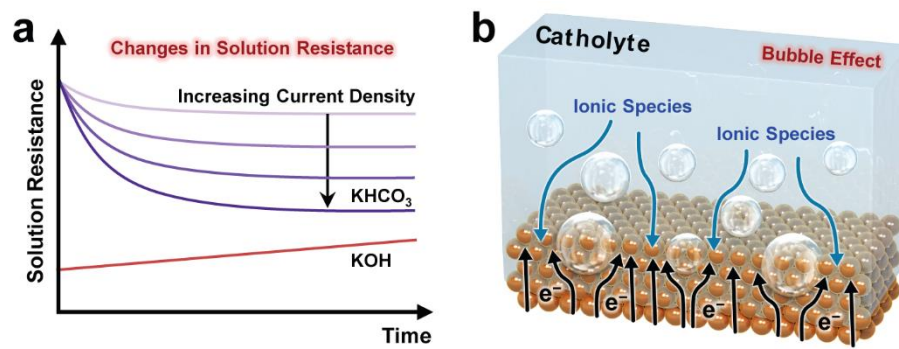


**Figure 5.** Common experimental pitfalls that can affect the determination of  $iR$ -corrected cathodic voltage in a GDE-based flow electrolyzers. (a) Changes in solution resistance over time for different electrolytes. (b) Bubble evolution from the catalyst layer affecting the actual electrochemically active surface area and the pathways of the ions.

Apart from the changes in solution resistance during the electrolysis, another factor that affects  $R_u$  is the formation of bubbles (Figure 5b). Considering that products such as  $\text{H}_2$ ,  $\text{CO}$ ,  $\text{CH}_4$  and  $\text{C}_2\text{H}_4$  have limited solubility in aqueous electrolytes, bubbles evolving from electrodes in the catholyte chamber could happen especially at high current densities, *i.e.* high product formation rate. Ideally, dissolved products should be formed near the gas-electrolyte-catalyst three-phase boundary, which enables selective evolution of gas products at the gas-liquid interfaces for facile transport toward the gas chamber. However, in practical situation, catalyst-electrolyte interfaces dominate the activities of  $\text{CO}_2$  conversion in a 3-dimensional catalyst layer, *i.e.* products are formed slightly away from the gas-electrolyte interface ( $< 10 \mu\text{m}$ ).<sup>34</sup> As a result, a portion of the product could nucleate and evolve as bubbles within the electrolyte-filled catalyst layer and escape through the catholyte chamber. The crossover of gas products to the catholyte is also a concern for the accurate quantification of products as discussed previously. The extent of bubble formation can be further aggravated if the GDE is overly wetted or flooded, which pushes the gas-electrolyte interface further away from the catalyst layer ( $> 10 \mu\text{m}$ ).<sup>74, 77</sup> Additionally, the crossover of gas reactant and products will be intensified if the pressure at the gas chamber is higher than that in the catholyte



chamber. For example, Legrand *et al.* reported that in their specified electrolyzer system, a pressure difference of more than 5 kPa would result in the undesired crossovers and thus formation of bubbles in the catholyte chambers.<sup>58</sup> Such pressure differences can be affected by a variety of factors, such as flow rates of CO<sub>2</sub> and catholyte, cell dimensions, etc., while the ease of gas/liquid crossovers is influenced by the pore size of GDEs, surface tension, viscosity of catholyte, etc.

Bubble evolution on the cathode surface would influence three types of overpotential (Figure 5b): (1) Additional ohmic overpotential would be observed due to the free and attached bubbles in the catholyte, which creates lengthier ion pathways for current transport. (2) Additional activation overpotential would also be resulted due to the attached bubbles masking the catalyst surfaces, which decreases the effective electrochemically active surface area. (3) A lower concentration overpotential could be observed as dissolved gas products can be more efficiently diffused and removed into the bubble, thus reducing supersaturation levels of products near the catalyst surfaces. The first type of bubble-induced overpotential effect, *i.e.* ohmic overpotential, would mean that  $R_u$  changes dynamically according to the nucleation and release of the gas products during CO<sub>2</sub> electrolysis. Therefore, we again emphasize that utilizing the pre-electrolysis  $R_u$  for voltage drop correction would not provide a meaningful working potential.

## PROTOCOLS

### Product FEs

Instead of assuming the gas effluent flow rate to be same as the feed flow rate, we emphasize that it is crucial for researchers to measure the effluent gas flow rate and report the method used for this measurement (electronic flowmeter, bubble flowmeter, etc.). Therefore, overestimation of gas product FEs can be avoided.

In order to account for the crossover of liquid products to the anode chamber, analyzing of liquid products in the anolyte should also be performed. However, there is also the possibility that the organic liquid products can be oxidized by the anode. Hence, several protocols have also been proposed to minimize the crossovers of liquid products to the anode chamber, such as the increase in catholyte flow rate and the replacement of AEM to cation-exchange membranes or bipolar membranes.<sup>43, 46, 47</sup> On the other hand, crossovers of volatile liquid products to the gas effluent can

be accounted by using a cold trap, or minimized by maintaining a low catholyte temperature and also increasing the volume of catholyte for circulation.<sup>48</sup>

To address for the loss of gas products through the catholyte effluent, Niu *et al.* recommended a protocol whereby the gas effluent of the GDE-based flow electrolyzer is bubbled into a gas-tight catholyte reservoir to mix with gas products escaping from the catholyte effluent.<sup>48</sup> The gas from the headspace of the catholyte reservoir are then fed to the GC for analysis. Although this protocol may help in redissolving part of the evaporated liquid products from the gas effluent back into the catholyte, there may also be other unintended effects, such as, further vaporization of the volatile products from the catholyte if the concentration or temperature is too high. Special care would also be needed to ensure minimal pressure build up in the gas chamber to overcome the hydrostatic pressure due to the immersion of gas outlet into the catholyte. When too much pressure is built up in the gas chamber, more gaseous products and reactants will crossover to the catholyte chamber.<sup>58</sup> An alternative solution would be to recover the evaporated volatile products with a cold trap before directing the gas effluent from the electrolyzer to the headspace of the catholyte reservoir.

Considering that microenvironments of catalyst surfaces can be altered by a wide range of experimental factors, it is important to report these experimental conditions: catholyte and CO<sub>2</sub> feed flow rate, preparation of catalyst layer (catalyst loading, ionomer loading, ink solvent, air-brushing conditions), etc. At the same time, commercially available standard catalysts, such as Cu nanopowder from Sigma-Aldrich, should be used as control samples for a more convenient comparison across literatures to verify the similarities/differences in microenvironment of the reported systems.

### **Cathodic Potentials**

Since  $R_u$  value would vary dynamically during CO<sub>2</sub> electrolysis due to changes in solution resistance and effects from bubble evolution, the following protocol is recommended to determine the  $iR$ -corrected working potential:

1. Perform chronopotentiometry without *in situ*  $R_u$  compensation from the potentiostat.
2. Determine  $R_u$  with impedance spectroscopy immediately after the chronopotentiometry ends.

3. Determine the  $iR$ -corrected working potential by using the final raw potential data point of the chronopotentiometry, specified current and the measured  $R_u$  (See Equation 2).
4. Perform Steps 1–3 consecutively for three times in a single run to obtain an average  $iR$ -corrected working potential.

Note that three independent runs using different electrode samples are still required to acquire the overall averaged  $iR$ -corrected working potential for each specified current density. However, applying a more accurate  $R_u$  value for voltage drop correction will not address the issues of bubble-induced activation and concentration overpotentials. Additional steps can be taken to minimize the extent of gas-masking of catalyst surfaces and bubble evolution in the catholyte chamber, such as reducing the pressure differences, optimizing the hydrophobicity/aerophobicity of catalyst layer, pre-designing bubble nucleation sites, etc.<sup>30, 77, 78</sup>

## SUMMARY AND OUTLOOK

GDE-based flow electrolyzers play an important role in bridging the gap between conventional electrochemical cells and industrial electrolyzers while allowing evaluation of catalysts possible. In the midst of rapid discoveries of the next-generation electrocatalysts, we emphasized in this Perspective the presence of various experimental factors that can influence the evaluation of CO<sub>2</sub>RR performances of the catalysts. Without addressing these pitfalls would result in inaccurate product FEs and cathodic potentials. Through a better awareness of these potential pitfalls and implementation of recommended protocols, we foresee a more meaningful comparison of catalytic properties across literatures and laboratories.<sup>36</sup> Consequently, a “cleaner” experimental database can be built, which enables a more reliable machine learning-enabled catalyst discovery. Nonetheless, the list of operational pitfalls and protocols for GDE-based electrolyzers discussed here should be continuously reviewed and refined as the development of CO<sub>2</sub>RR continues to evolve. For example, the following topics will require further discussion and alignment among the research community:

- Experimental conditions for the measurement of electrochemically active surface area. The limitation of the commonly used method depends on double layer capacitance, which changes based on the extent of wetness of the porous GDE substrate.<sup>79</sup>
- Experimental conditions of flow electrolyzer with bipolar membranes for CO<sub>2</sub>RR.<sup>80, 81</sup>

- Experimental conditions for acidic CO<sub>2</sub>RR.<sup>67</sup>
- Experimental conditions for the coupling of CO<sub>2</sub>RR with N<sub>2</sub>/NO<sub>x</sub>/NO<sub>2</sub><sup>-</sup>/NO<sub>3</sub><sup>-</sup> reduction reaction.<sup>82, 83</sup>
- Experimental conditions and reactor design of GDE-based flow electrolyzers for *in situ* characterizations, such as surface-enhanced Raman spectroscopy and X-ray absorption spectroscopy.<sup>84, 85</sup>

Apart from three-compartment GDE-based flow electrolyzers, MEA electrolyzers also deserve more attention for establishing appropriate experimental protocols as it is still the most industrially relevant electrolyzer that can be employed in laboratories. Among the experimental pitfalls that are highlighted in this Perspective, not all of them are applicable to MEA systems. For example, *iR*-correction is not required as full-cell voltage are typically reported, hence the dynamic change of  $R_u$  will not matter. Also, the loss of gas products through bubble formation will not occur as solid electrolytes are used, and the loss of volatile liquid products through gas effluent are usually anticipated and collected with the typical cold trap connected to the outlet of MEA. Nonetheless, MEA electrolyzer systems present a more complex range of operational challenges.<sup>37, 72, 86-88</sup> We encourage further dialogues and provision of experimental guidelines to address foreseeable pitfalls that researchers would face in these fields, hence further accelerating the progress of CO<sub>2</sub>RR toward commercialization.

#### ASSOCIATED CONTENT

**Supporting Information.** The Supporting Information is available free of charge at

Data points and references used for the plot in Figure 1a (Table S1).

#### AUTHOR INFORMATION

**Ying Chuan Tan** – Institute of Materials Research and Engineering (IMRE), A\*STAR, 2 Fusionopolis Way, #08-03 Innovis, Singapore 138634, Singapore; Institute of Sustainability for Chemicals, Energy and Environment (ISCE2), A\*STAR, 1 Pesek Road, Jurong Island, Singapore 627833, Singapore; [orcid.org/0000-0003-3281-0350](https://orcid.org/0000-0003-3281-0350)

**Wei Kang Quek** – Department of Material Science Engineering, National University of Singapore, 9 Engineering Drive 1, #03-09 EA, Singapore 117575, Singapore

**Beomil Kim** – Department of Materials Science and Engineering, Korea Advanced Institute of Science and Technology (KAIST), 291 Daehak-ro, Yuseong-gu, Daejeon 34141, Republic of Korea; [orcid.org/0000-0002-3247-0205](https://orcid.org/0000-0002-3247-0205)

**Sigit Sugiarto** – Institute of Materials Research and Engineering (IMRE), A\*STAR, 2 Fusionopolis Way, #08-03 Innovis, Singapore 138634, Singapore

**Jihun Oh** – Department of Materials Science and Engineering, Korea Advanced Institute of Science and Technology (KAIST), 291 Daehak-ro, Yuseong-gu, Daejeon 34141, Republic of Korea; [orcid.org/0000-0001-6465-6736](https://orcid.org/0000-0001-6465-6736)

**Dan Kai** – Institute of Materials Research and Engineering (IMRE), A\*STAR, 2 Fusionopolis Way, #08-03 Innovis, Singapore 138634, Singapore; Institute of Sustainability for Chemicals, Energy and Environment (ISCE2), A\*STAR, 1 Pesek Road, Jurong Island, Singapore 627833, Singapore; [orcid.org/0000-0002-2330-3480](https://orcid.org/0000-0002-2330-3480)

## Notes

The authors declare no competing financial interest.

## Biographies

Ying Chuan Tan is a Research Scientist at the Institute of Materials Research and Engineering, and the Institute of Sustainability for Chemicals, Energy and Environment. He received his Ph.D. from National University of Singapore in 2018. His research focuses on the design of nanocatalysts and gas-diffusion electrodes for CO<sub>2</sub> electroreduction.

Wei Kang Quek is an undergraduate researcher attached to the Institute of Materials Research and Engineering while pursuing his B.Eng. in Materials Science and Engineering at National University of Singapore. His research interests include the conversion of biomass materials and the synthesis of nanocatalysts for CO<sub>2</sub> electroreduction.

Beomil Kim is a Ph.D. candidate in the Department of Materials Science and Engineering at Korea Advanced Institute of Science and Technology (KAIST). He received his M.S. in Materials Science and Engineering from KAIST in 2019. His research focuses on developing systems and catalysts for CO<sub>2</sub> electroreduction.

Sigit Sugiarto is a research specialist at the Institute of Materials Research and Engineering. He received his B.Sc. in Chemistry from National University of Singapore in 2017. Presently, he is

working on the chemical functionalization of biomass-derived molecules for the development of bio-materials with enhanced properties.

Jihun Oh is an Associate Professor in the Department of Materials Science and Engineering at the Korea Advanced Institute of Science and Technology in Republic of Korea. His research interests include understanding and designing materials for (photo)electrocatalytic CO<sub>2</sub> and N<sub>2</sub> reduction and biomass upgrade. <http://les.kaist.ac.kr/index.php>

Dan Kai is a Research Scientist and Group Leader at the Institute of Materials Research and Engineering, and the Institute of Sustainability for Chemicals, Energy and Environment. His research interests include sustainable materials, biomass valorization, low carbon technologies and biomedical engineering.

## ACKNOWLEDGMENT

Y.C.T., S.S. and K.D. gratefully acknowledge the financial support by the Agency for Science, Technology and Research (A\*STAR) under its Career Development Fund (CDF 202D800033). B.K. and J.O acknowledge the financial support provided by the National Research Foundation of Korea (NRF-2021R1A2C3007280) and the “Carbon to X Project” (NRF-2020M3H7A1096388) through the National Research Foundation (NRF) of the Republic of Korea.

## REFERENCES

1. Nitopi, S.; Bertheussen, E.; Scott, S. B.; Liu, X.; Engstfeld, A. K.; Horch, S.; Seger, B.; Stephens, I. E. L.; Chan, K.; Hahn, C., et al., Progress and Perspectives of Electrochemical Co<sub>2</sub> Reduction on Copper in Aqueous Electrolyte. *Chem. Rev.* **2019**, *119* (12), 7610-7672.
2. Jordaan, S. M.; Wang, C., Electrocatalytic Conversion of Carbon Dioxide for the Paris Goals. *Nat. Catal.* **2021**, *4* (11), 915-920.
3. Hauch, A.; Kungas, R.; Blennow, P.; Hansen, A. B.; Hansen, J. B.; Mathiesen, B. V.; Mogensen, M. B., Recent Advances in Solid Oxide Cell Technology for Electrolysis. *Science* **2020**, *370* (6513).
4. De Luna, P.; Hahn, C.; Higgins, D.; Jaffer, S. A.; Jaramillo, T. F.; Sargent, E. H., What Would It Take for Renewably Powered Electrosynthesis to Displace Petrochemical Processes? *Science* **2019**, *364* (6438).
5. Kungas, R., Review—Electrochemical Co<sub>2</sub> Reduction for Co Production: Comparison of Low- and High-Temperature Electrolysis Technologies. *J. Electrochem. Soc.* **2020**, *167* (4).
6. Karapinar, D.; Creissen, C. E.; Rivera de la Cruz, J. G.; Schreiber, M. W.; Fontecave, M., Electrochemical Co<sub>2</sub> Reduction to Ethanol with Copper-Based Catalysts. *ACS Energy Lett.* **2021**, *6* (2), 694-706.

7. Gao, D.; Arán-Ais, R. M.; Jeon, H. S.; Roldan Cuenya, B., Rational Catalyst and Electrolyte Design for Co<sub>2</sub> Electroreduction Towards Multicarbon Products. *Nat. Catal.* **2019**, *2* (3), 198-210.
8. Sun, Z.; Hu, Y.; Zhou, D.; Sun, M.; Wang, S.; Chen, W., Factors Influencing the Performance of Copper-Bearing Catalysts in the Co<sub>2</sub> Reduction System. *ACS Energy Lett.* **2021**, *6* (11), 3992-4022.
9. Song, H.; Tan, Y. C.; Kim, B.; Ringe, S.; Oh, J., Tunable Product Selectivity in Electrochemical Co<sub>2</sub> Reduction on Well-Mixed Ni-Cu Alloys. *ACS Appl. Mater. Interfaces* **2021**, *13* (46), 55272-55280.
10. Resasco, J.; Bell, A. T., Electrocatalytic Co<sub>2</sub> Reduction to Fuels: Progress and Opportunities. *Trends in Chemistry* **2020**, *2* (9), 825-836.
11. Wakerley, D.; Lamaison, S.; Wicks, J.; Clemens, A.; Feaster, J.; Corral, D.; Jaffer, S. A.; Sarkar, A.; Fontecave, M.; Duoss, E. B., et al., Gas Diffusion Electrodes, Reactor Designs and Key Metrics of Low-Temperature Co<sub>2</sub> Electrolysers. *Nat. Energy* **2022**, *7* (2), 130-143.
12. Govindarajan, N.; Kastlunger, G.; Heenen, H. H.; Chan, K., Improving the Intrinsic Activity of Electrocatalysts for Sustainable Energy Conversion: Where Are We and Where Can We Go? *Chem Sci* **2021**, *13* (1), 14-26.
13. Higgins, D.; Hahn, C.; Xiang, C.; Jaramillo, T. F.; Weber, A. Z., Gas-Diffusion Electrodes for Carbon Dioxide Reduction: A New Paradigm. *ACS Energy Lett.* **2019**, *4* (1), 317-324.
14. Nguyen, T. N.; Dinh, C.-T., Gas Diffusion Electrode Design for Electrochemical Carbon Dioxide Reduction. *Chem. Soc. Rev.* **2020**, *49* (21), 7488-7504.
15. Shin, H.; Hansen, K. U.; Jiao, F., Techno-Economic Assessment of Low-Temperature Carbon Dioxide Electrolysis. *Nat. Sustain.* **2021**, *4* (10), 911-919.
16. Lees, E. W.; Mowbray, B. A. W.; Parlange, F. G. L.; Berlinguette, C. P., Gas Diffusion Electrodes and Membranes for Co<sub>2</sub> Reduction Electrolysers. *Nat. Rev. Mater.* **2021**.
17. Abbas, S. A.; Song, J. T.; Tan, Y. C.; Nam, K. M.; Oh, J.; Jung, K.-D., Synthesis of a Nickel Single-Atom Catalyst Based on Ni–N<sub>4</sub>–Xcx Active Sites for Highly Efficient Co<sub>2</sub> Reduction Utilizing a Gas Diffusion Electrode. *ACS Appl. Energy Mater.* **2020**, *3* (9), 8739-8745.
18. Choi, B.-U.; Tan, Y. C.; Song, H.; Lee, K. B.; Oh, J., System Design Considerations for Enhancing Electroproduction of Formate from Simulated Flue Gas. *ACS Sustain. Chem. Eng.* **2021**, *9* (5), 2348-2357.
19. Burdyny, T.; Smith, W. A., Co<sub>2</sub> Reduction on Gas-Diffusion Electrodes and Why Catalytic Performance Must Be Assessed at Commercially-Relevant Conditions. *Energy Environ. Sci.* **2019**, *12* (5), 1442-1453.
20. Kim, B.; Seong, H.; Song, J. T.; Kwak, K.; Song, H.; Tan, Y. C.; Park, G.; Lee, D.; Oh, J., Over a 15.9% Solar-to-Co Conversion from Dilute Co<sub>2</sub> Streams Catalyzed by Gold Nanoclusters Exhibiting a High Co<sub>2</sub> Binding Affinity. *ACS Energy Lett.* **2019**, *5* (3), 749-757.
21. Jeong, G. H.; Tan, Y. C.; Song, J. T.; Lee, G.-Y.; Lee, H. J.; Lim, J.; Jeong, H. Y.; Won, S.; Oh, J.; Kim, S. O., Synthetic Multiscale Design of Nanostructured Ni Single Atom Catalyst for Superior Co<sub>2</sub> Electroreduction. *Chemical Engineering Journal* **2021**, 426.
22. Ma, W.; Xie, S.; Liu, T.; Fan, Q.; Ye, J.; Sun, F.; Jiang, Z.; Zhang, Q.; Cheng, J.; Wang, Y., Electrocatalytic Reduction of Co<sub>2</sub> to Ethylene and Ethanol through Hydrogen-Assisted C–C Coupling over Fluorine-Modified Copper. *Nat. Catal.* **2020**, *3* (6), 478-487.

23. García de Arquer, F. P.; Dinh, C. T.; Ozden, A.; Wicks, J.; McCallum, C.; Kirmani, A.; Nam, D.-H.; Gabardo, C.; Seifitokaldani, A.; Wang, X., et al., Co<sub>2</sub> Electrolysis to Multicarbon Products at Activities Greater Than 1 a Cm<sup>-2</sup>. *Science* **2020**, *367*, 661-666.
24. Li, Y.; Xu, A.; Lum, Y.; Wang, X.; Hung, S. F.; Chen, B.; Wang, Z.; Xu, Y.; Li, F.; Abed, J., et al., Promoting Co<sub>2</sub> Methanation Via Ligand-Stabilized Metal Oxide Clusters as Hydrogen-Donating Motifs. *Nat. Commun.* **2020**, *11* (1), 6190.
25. Li, F.; Li, Y. C.; Wang, Z.; Li, J.; Nam, D.-H.; Lum, Y.; Luo, M.; Wang, X.; Ozden, A.; Hung, S.-F., et al., Cooperative Co<sub>2</sub>-to-Ethanol Conversion Via Enriched Intermediates at Molecule–Metal Catalyst Interfaces. *Nat. Catal.* **2019**, *3* (1), 75-82.
26. Sedighian Rasouli, A.; Wang, X.; Wicks, J.; Lee, G.; Peng, T.; Li, F.; McCallum, C.; Dinh, C.-T.; Ip, A. H.; Sinton, D., et al., Co<sub>2</sub> Electroreduction to Methane at Production Rates Exceeding 100 Ma/Cm<sup>2</sup>. *ACS Sustain. Chem. Eng.* **2020**, *8* (39), 14668-14673.
27. Li, F.; Thevenon, A.; Rosas-Hernández, A.; Wang, Z.; Li, Y.; Gabardo, C. M.; Ozden, A.; Dinh, C. T.; Li, J.; Wang, Y., et al., Molecular Tuning of Co<sub>2</sub>-to-Ethylene Conversion. *Nature* **2020**, *577* (7791), 509-513.
28. Liu, K.; Smith, W. A.; Burdyny, T., Introductory Guide to Assembling and Operating Gas Diffusion Electrodes for Electrochemical Co<sub>2</sub> Reduction. *ACS Energy Lett.* **2019**, *4* (3), 639-643.
29. Ma, M.; Clark, E. L.; Therkildsen, K. T.; Dalsgaard, S.; Chorkendorff, I.; Seger, B., Insights into the Carbon Balance for Co<sub>2</sub> Electroreduction on Cu Using Gas Diffusion Electrode Reactor Designs. *Energy Environ. Sci.* **2020**, *13* (3), 977-985.
30. Angulo, A.; van der Linde, P.; Gardeniers, H.; Modestino, M.; Fernández Rivas, D., Influence of Bubbles on the Energy Conversion Efficiency of Electrochemical Reactors. *Joule* **2020**, *4* (3), 555-579.
31. Hernandez-Aldave, S.; Andreoli, E., Fundamentals of Gas Diffusion Electrodes and Electrolysers for Carbon Dioxide Utilisation: Challenges and Opportunities. *Catalysts* **2020**, *10* (6).
32. Weekes, D. M.; Salvatore, D. A.; Reyes, A.; Huang, A.; Berlinguette, C. P., Electrolytic Co<sub>2</sub> Reduction in a Flow Cell. *Acc. Chem. Res.* **2018**, *51* (4), 910-918.
33. Moore, T.; Xia, X.; Baker, S. E.; Duoss, E. B.; Beck, V. A., Elucidating Mass Transport Regimes in Gas Diffusion Electrodes for Co<sub>2</sub> Electroreduction. *ACS Energy Lett.* **2021**, *6* (10), 3600-3606.
34. Nesbitt, N. T.; Burdyny, T.; Simonson, H.; Salvatore, D.; Bohra, D.; Kas, R.; Smith, W. A., Liquid–Solid Boundaries Dominate Activity of Co<sub>2</sub> Reduction on Gas-Diffusion Electrodes. *ACS Catal.* **2020**, *10* (23), 14093-14106.
35. Weng, L. C.; Bell, A. T.; Weber, A. Z., Modeling Gas-Diffusion Electrodes for Co<sub>2</sub> Reduction. *Phys. Chem. Chem. Phys.* **2018**, *20* (25), 16973-16984.
36. Ehelebe, K.; Schmitt, N.; Sievers, G.; Jensen, A. W.; Hrnjić, A.; Collantes Jiménez, P.; Kaiser, P.; Geuß, M.; Ku, Y.-P.; Jovanović, P., et al., Benchmarking Fuel Cell Electrocatalysts Using Gas Diffusion Electrodes: Inter-Lab Comparison and Best Practices. *ACS Energy Lett.* **2022**, *7* (2), 816-826.
37. Salvatore, D.; Berlinguette, C. P., Voltage Matters When Reducing Co<sub>2</sub> in an Electrochemical Flow Cell. *ACS Energy Lett.* **2019**, *5* (1), 215-220.
38. Song, H.; Song, J. T.; Kim, B.; Tan, Y. C.; Oh, J., Activation of C<sub>2</sub>H<sub>4</sub> Reaction Pathways in Electrochemical Co<sub>2</sub> Reduction under Low Co<sub>2</sub> Partial Pressure. *Applied Catalysis B: Environmental* **2020**, 272.



39. Yang, K.; Kas, R.; Smith, W. A.; Burdyny, T., Role of the Carbon-Based Gas Diffusion Layer on Flooding in a Gas Diffusion Electrode Cell for Electrochemical Co<sub>2</sub> Reduction. *ACS Energy Lett.* **2021**, *6* (1), 33-40.
40. Lv, J.-J.; Jouny, M.; Luc, W.; Zhu, W.; Zhu, J.-J.; Jiao, F., A Highly Porous Copper Electrocatalyst for Carbon Dioxide Reduction. *Adv. Mater.* **2018**, *30* (49), 1803111.
41. Dinh, C.-T.; Burdyny, T.; Kibria, M. G.; Seifitokaldani, A.; Gabardo, C. M.; García de Arquer, F. P.; Kiani, A.; Edwards, J. P.; De Luna, P.; Bushuyev, O. S., et al., Co<sub>2</sub> Electroreduction to Ethylene Via Hydroxide-Mediated Copper Catalysis at an Abrupt Interface. *Science* **2018**, *360* (6390).
42. Tan, Y. C.; Lee, K. B.; Song, H.; Oh, J., Modulating Local Co<sub>2</sub> Concentration as a General Strategy for Enhancing C–C Coupling in Co<sub>2</sub> Electroreduction. *Joule* **2020**, *4* (5), 1104-1120.
43. Larrazábal, G. O.; Ma, M.; Seger, B., A Comprehensive Approach to Investigate Co<sub>2</sub> Reduction Electrocatalysts at High Current Densities. *Acc. Mater. Res.* **2021**, *2* (4), 220-229.
44. Rabinowitz, J. A.; Kanan, M. W., The Future of Low-Temperature Carbon Dioxide Electrolysis Depends on Solving One Basic Problem. *Nat. Commun.* **2020**, *11* (1), 5231.
45. Li, J.; Wu, D.; Malkani, A. S.; Chang, X.; Cheng, M. J.; Xu, B.; Lu, Q., Hydroxide Is Not a Promoter of C<sub>2</sub><sup>+</sup> Product Formation in the Electrochemical Reduction of Co on Copper. *Angew. Chem. Int. Ed.* **2020**, *59* (11), 4464-4469.
46. Zhang, J.; Luo, W.; Züttel, A., Crossover of Liquid Products from Electrochemical Co<sub>2</sub> Reduction through Gas Diffusion Electrode and Anion Exchange Membrane. *J. Catal.* **2020**, *385*, 140-145.
47. Ma, M.; Kim, S.; Chorkendorff, I.; Seger, B., Role of Ion-Selective Membranes in the Carbon Balance for Co<sub>2</sub> Electroreduction Via Gas Diffusion Electrode Reactor Designs. *Chem Sci* **2020**, *11* (33), 8854-8861.
48. Niu, Z.-Z.; Chi, L.-P.; Liu, R.; Chen, Z.; Gao, M.-R., Rigorous Assessment of Co<sub>2</sub> Electroreduction Products in a Flow Cell. *Energy Environ. Sci.* **2021**, *14* (8), 4169-4176.
49. Wagner, A.; Sahn, C. D.; Reisner, E., Towards Molecular Understanding of Local Chemical Environment Effects in Electro- and Photocatalytic Co<sub>2</sub> Reduction. *Nat. Catal.* **2020**, *3* (10), 775-786.
50. Gao, D.; Scholten, F.; Roldan Cuenya, B., Improved Co<sub>2</sub> Electroreduction Performance on Plasma-Activated Cu Catalysts Via Electrolyte Design: Halide Effect. *ACS Catal.* **2017**, *7* (8), 5112-5120.
51. Ringe, S.; Clark, E. L.; Resasco, J.; Walton, A.; Seger, B.; Bell, A. T.; Chan, K., Understanding Cation Effects in Electrochemical Co<sub>2</sub> Reduction. *Energy Environ. Sci.* **2019**, *12* (10), 3001-3014.
52. Murata, A.; Hori, Y., Product Selectivity Affected by Cationic Species in Electrochemical Reduction of Co<sub>2</sub> and Co at a Cu Electrode. *Bulletin of the Chemical Society of Japan* **1991**, *64* (1), 123-127.
53. Kas, R.; Kortlever, R.; Yilmaz, H.; Koper, M. T.; Mul, G., Manipulating the Hydrocarbon Selectivity of Copper Nanoparticles in Co<sub>2</sub> Electroreduction by Process Conditions. *ChemElectroChem* **2015**, *2* (3), 354-358.
54. Resasco, J.; Lum, Y.; Clark, E.; Zeledon, J. Z.; Bell, A. T., Effects of Anion Identity and Concentration on Electrochemical Reduction of Co<sub>2</sub>. *ChemElectroChem* **2018**, *5* (7), 1064-1072.

55. Resasco, J.; Chen, L. D.; Clark, E.; Tsai, C.; Hahn, C.; Jaramillo, T. F.; Chan, K.; Bell, A. T., Promoter Effects of Alkali Metal Cations on the Electrochemical Reduction of Carbon Dioxide. *Journal of the American Chemical Society* **2017**, *139* (32), 11277-11287.
56. Wuttig, A.; Yaguchi, M.; Motobayashi, K.; Osawa, M.; Surendranath, Y., Inhibited Proton Transfer Enhances Au-Catalyzed Co<sub>2</sub>-to-Fuels Selectivity. *Proc. Natl. Acad. Sci. U.S.A.* **2016**, *113* (32), E4585-E4593.
57. Bhargava, S. S.; Proietto, F.; Azmoodeh, D.; Cofell, E. R.; Henckel, D. A.; Verma, S.; Brooks, C. J.; Gewirth, A. A.; Kenis, P. J. A., System Design Rules for Intensifying the Electrochemical Reduction of Co<sub>2</sub> to Co on Ag Nanoparticles. *ChemElectroChem* **2020**, *7* (9), 2001-2011.
58. Legrand, U.; Lee, J. K.; Bazylak, A.; Tavares, J. R., Product Crossflow through a Porous Gas Diffusion Layer in a Co<sub>2</sub> Electrochemical Cell with Pressure Drop Calculations. *Ind. Eng. Chem. Res.* **2021**, *60* (19), 7187-7196.
59. Van Daele, K.; De Mot, B.; Pupo, M.; Daems, N.; Pant, D.; Kortlever, R.; Breugelmans, T., Sn-Based Electrocatalyst Stability: A Crucial Piece to the Puzzle for the Electrochemical Co<sub>2</sub> Reduction toward Formic Acid. *ACS Energy Lett.* **2021**, *6* (12), 4317-4327.
60. Nwabara, U. O.; Cofell, E. R.; Verma, S.; Negro, E.; Kenis, P. J. A., Durable Cathodes and Electrolyzers for the Efficient Aqueous Electrochemical Reduction of Co<sub>2</sub>. *ChemSusChem* **2020**, *13* (5), 855-875.
61. Wu, Y.; Garg, S.; Li, M.; Idros, M. N.; Li, Z.; Lin, R.; Chen, J.; Wang, G.; Rufford, T. E., Effects of Microporous Layer on Electrolyte Flooding in Gas Diffusion Electrodes and Selectivity of Co<sub>2</sub> Electrolysis to Co. *Journal of Power Sources* **2022**, 522.
62. Kovalev, M. K.; Ren, H.; Zakir Muhamad, M.; Ager, J. W.; Lapkin, A. A., Minor Product Polymerization Causes Failure of High-Current Co<sub>2</sub>-to-Ethylene Electrolyzers. *ACS Energy Lett.* **2022**, 599-601.
63. Xu, Y.; Edwards, J. P.; Liu, S.; Miao, R. K.; Huang, J. E.; Gabardo, C. M.; O'Brien, C. P.; Li, J.; Sargent, E. H.; Sinton, D., Self-Cleaning Co<sub>2</sub> Reduction Systems: Unsteady Electrochemical Forcing Enables Stability. *ACS Energy Lett.* **2021**, *6* (2), 809-815.
64. Endrődi, B.; Samu, A.; Kecsenovity, E.; Halmágyi, T.; Sebők, D.; Janáky, C., Operando Cathode Activation with Alkali Metal Cations for High Current Density Operation of Water-Fed Zero-Gap Carbon Dioxide Electrolysers. *Nat. Energy* **2021**, *6* (4), 439-448.
65. Monteiro, M. C. O.; Dattila, F.; Hagedoorn, B.; García-Muelas, R.; López, N.; Koper, M. T. M., Absence of Co<sub>2</sub> Electroreduction on Copper, Gold and Silver Electrodes without Metal Cations in Solution. *Nat. Catal.* **2021**, *4* (8), 654-662.
66. Bondue, C. J.; Graf, M.; Goyal, A.; Koper, M. T. M., Suppression of Hydrogen Evolution in Acidic Electrolytes by Electrochemical Co<sub>2</sub> Reduction. *J. Am. Chem. Soc.* **2021**, *143* (1), 279-285.
67. Huang, J. E.; Li, F.; Ozden, A.; Sedighian Rasouli, A.; García de Arquer, F. P.; Liu, S.; Zhang, S.; Luo, M.; Wang, X.; Lum, Y., et al., Co<sub>2</sub> Electrolysis to Multicarbon Products in Strong Acid. *Science* **2021**, *372* (6546), 1074.
68. Jouny, M.; Hutchings, G. S.; Jiao, F., Carbon Monoxide Electroreduction as an Emerging Platform for Carbon Utilization. *Nat. Catal.* **2019**, *2* (12), 1062-1070.
69. Sandberg, R. B.; Montoya, J. H.; Chan, K.; Nørskov, J. K., Co-Co Coupling on Cu Facets: Coverage, Strain and Field Effects. *Surf. Sci.* **2016**, *654*, 56-62.

70. Fenwick, A. Q.; Welch, A. J.; Li, X.; Sullivan, I.; DuChene, J. S.; Xiang, C.; Atwater, H. A., Probing the Catalytically Active Region in a Nanoporous Gold Gas Diffusion Electrode for Highly Selective Carbon Dioxide Reduction. *ACS Energy Lett.* **2022**, 871-879.
71. Mowbray, B. A. W.; Dvorak, D. J.; Taherimakhsoosi, N.; Berlinguette, C. P., How Catalyst Dispersion Solvents Affect Co<sub>2</sub> Electrolyzer Gas Diffusion Electrodes. *Energy Fuels* **2021**, 35 (23), 19178-19184.
72. Möller, T.; Ngo Thanh, T.; Wang, X.; Ju, W.; Jovanov, Z.; Strasser, P., The Product Selectivity Zones in Gas Diffusion Electrodes During the Electrocatalytic Reduction of Co<sub>2</sub>. *Energy Environ. Sci.* **2021**, 14 (11), 5995-6006.
73. Lees, E. W.; Mowbray, B. A. W.; Salvatore, D. A.; Simpson, G. L.; Dvorak, D. J.; Ren, S.; Chau, J.; Milton, K. L.; Berlinguette, C. P., Linking Gas Diffusion Electrode Composition to Co<sub>2</sub> Reduction in a Flow Cell. *J. Mater. Chem. A* **2020**, 8 (37), 19493-19501.
74. Bienen, F.; Hildebrand, J.; Kopljar, D.; Wagner, N.; Klemm, E.; Friedrich, K. A., Importance of Time-Dependent Wetting Behavior of Gas-Diffusion Electrodes for Reactivity Determination *Chem. Ing. Tech.* **2021**, 93 (6), 1015-1019.
75. Kim, C.; Bui, J. C.; Luo, X.; Cooper, J. K.; Kusoglu, A.; Weber, A. Z.; Bell, A. T., Tailored Catalyst Microenvironments for Co<sub>2</sub> Electroreduction to Multicarbon Products on Copper Using Bilayer Ionomer Coatings. *Nat. Energy* **2021**, 6 (11), 1026-1034.
76. Clark, E. L.; Resasco, J.; Landers, A.; Lin, J.; Chung, L.-T.; Walton, A.; Hahn, C.; Jaramillo, T. F.; Bell, A. T., Standards and Protocols for Data Acquisition and Reporting for Studies of the Electrochemical Reduction of Carbon Dioxide. *ACS Catal.* **2018**, 8 (7), 6560-6570.
77. Li, M.; Idros, M. N.; Wu, Y.; Burdyny, T.; Garg, S.; Zhao, X. S.; Wang, G.; Rufford, T. E., The Role of Electrode Wettability in Electrochemical Reduction of Carbon Dioxide. *J. Mater. Chem. A* **2021**, 9 (35), 19369-19409.
78. Chen, R.; Tian, W.; Jia, Y.; Xu, W.; Chen, F.; Duan, X.; Xie, Q.; Hu, C.; Liu, W.; Zhao, Y., et al., Engineering Interfacial Aerophilicity of Nickel-Embedded Nitrogen-Doped Cnts for Electrochemical Co<sub>2</sub> Reduction. *ACS Appl. Energy Mater.* **2019**, 2 (6), 3991-3998.
79. Leonard, M. E.; Clarke, L. E.; Forner-Cuenca, A.; Brown, S. M.; Brushett, F. R., Investigating Electrode Flooding in a Flowing Electrolyte, Gas-Fed Carbon Dioxide Electrolyzer. *ChemSusChem* **2020**, 13 (2), 400-411.
80. Yang, K.; Li, M.; Subramanian, S.; Blommaert, M. A.; Smith, W. A.; Burdyny, T., Cation-Driven Increases of Co<sub>2</sub> Utilization in a Bipolar Membrane Electrode Assembly for Co<sub>2</sub> Electrolysis. *ACS Energy Lett.* **2021**, 6 (12), 4291-4298.
81. Blommaert, M. A.; Aili, D.; Tufa, R. A.; Li, Q.; Smith, W. A.; Vermaas, D. A., Insights and Challenges for Applying Bipolar Membranes in Advanced Electrochemical Energy Systems. *ACS Energy Lett.* **2021**, 6 (7), 2539-2548.
82. Chen, C.; Zhu, X.; Wen, X.; Zhou, Y.; Zhou, L.; Li, H.; Tao, L.; Li, Q.; Du, S.; Liu, T., et al., Coupling N<sub>2</sub> and Co<sub>2</sub> in H<sub>2</sub>O to Synthesize Urea under Ambient Conditions. *Nat Chem* **2020**, 12 (8), 717-724.
83. Kamat, P.; Christopher, P., Gas Diffusion Electrodes for Co<sub>2</sub> and N<sub>2</sub> Reduction: A Virtual Issue. *ACS Energy Lett.* **2022**, 1469-1472.
84. Firet, N. J.; Burdyny, T.; Nesbitt, N. T.; Chandrashekar, S.; Longo, A.; Smith, W. A., Copper and Silver Gas Diffusion Electrodes Performing Co<sub>2</sub> Reduction Studied through Operando X-Ray Absorption Spectroscopy. *Catalysis Science & Technology* **2020**, 10 (17), 5870-5885.

85. Wang, X.; Wang, Z.; García de Arquer, F. P.; Dinh, C.-T.; Ozden, A.; Li, Y. C.; Nam, D.-H.; Li, J.; Liu, Y.-S.; Wicks, J., et al., Efficient Electrically Powered Co<sub>2</sub>-to-Ethanol Via Suppression of Deoxygenation. *Nat. Energy* **2020**, *5* (6), 478-486.
86. Reyes, A.; Jansson, R. P.; Mowbray, B. A. W.; Cao, Y.; Wheeler, D. G.; Chau, J.; Dvorak, D. J.; Berlinguette, C. P., Managing Hydration at the Cathode Enables Efficient Co<sub>2</sub> Electrolysis at Commercially Relevant Current Densities. *ACS Energy Lett.* **2020**, *5* (5), 1612-1618.
87. Xia, C.; Zhu, P.; Jiang, Q.; Pan, Y.; Liang, W.; Stavitski, E.; Alshareef, H. N.; Wang, H., Continuous Production of Pure Liquid Fuel Solutions Via Electrocatalytic Co<sub>2</sub> Reduction Using Solid-Electrolyte Devices. *Nat. Energy* **2019**, *4* (9), 776-785.
88. Xu, Q.; Oener, S. Z.; Lindquist, G.; Jiang, H.; Li, C.; Boettcher, S. W., Integrated Reference Electrodes in Anion-Exchange-Membrane Electrolyzers: Impact of Stainless-Steel Gas-Diffusion Layers and Internal Mechanical Pressure. *ACS Energy Lett.* **2020**, *6* (2), 305-312.